Tunable Broadband Chaotic Signal Synthesis From a WRC-FPLD Subject to Filtered Feedback

Zhu-Qiang Zhong, Gong-Ru Lin, Zheng-Mao Wu, Ji-Yun Yang, Jian-Jun Chen, Li-Lin Yi, and Guang-Qiong Xia

Abstract—The synthesis of wavelength-tunable broadband chaotic signals is experimentally demonstrated by using a weak-resonant-cavity Fabry–Perot laser diode (WRC-FPLD) subject to filtered feedback. To perform the broadband tunability from 1544 to 1556 nm, a tunable optical filter is used for providing filtered feedback to drive the laser into chaos. With adjusting the central wavelength of the filter, about 20 longitudinal modes of the WRC-FPLD can individually realize the chaotic output within the tunable range of the filter. Moreover, by suitably selecting the feedback power, the chaos signal with a flat power spectrum and broad bandwidth up to ∼30.0 GHz can be achieved.

Index Terms—Weak-resonant-cavity Fabry-Perot laser diode (WRC-FPLD), chaotic signal, filtered feedback, wavelength tunable, broadband.

I. INTRODUCTION

OPTICAL chaos based on semiconductor lasers (SLs) has attracted intensive attention for its widespread applications [1] in fast random number generation [2]–[4], chaotic lidar [5], and especially chaos-based optical communications [6]–[11] due to good compatibility with existing optical fiber networks. In chaos-based optical communications, noise-like optical chaotic signals are employed as carriers to encrypt the messages at the transmitter and then subtracted at the receiver to recover the messages based on chaos synchronization. To strengthen the physical security and improve the data transmission rate, many efforts have been devoted to seeking highly dynamical complexity and broad bandwidth of chaotic carriers [12]–[15].

In recent years, wavelength division multiplex (WDM) schemes have been introduced to chaos-based optical communication [16]–[20]. Zhang *et al.* [16] theoretically investigated the WDM transmission of chaotic optical communication (COC) and conventional fiber-optic communication (CFOC), and discussed the inter-channel crosstalk of COC and CFOC. By adopting two chaotic optical injected multimode SLs, Jiang *et al.* [17] theoretically studied a physically enhanced secure WDM chaos communication system. Besides, some experimental works have also been

Z.-Q. Zhong, Z.-M. Wu, J.-Y. Yang, J.-J. Chen, and G.-Q. Xia are with the School of Physical Science and Technology, Southwest University, Chongqing 400715, China (e-mail: zmwu@swu.edu.cn; gqxia@swu.edu.cn).

G.-R. Lin is with the Graduate Institute of Photonics and Optoelectronics, National Taiwan University, Taipei 10617, Taiwan (e-mail: grlin@ntu.edu.tw).

L.-L. Yi is with the State Key Lab of Advanced Communication Systems and Networks, Shanghai Jiao Tong University, Shanghai 200240, China.

reported successively [18]–[20]. Paul *et al.* [18] experimentally demonstrated two channels chaotic optical communication by using two external-cavity laser diodes to generate dual-channel chaotic carriers. Matsuura *et al.* [19] studied chaotic WDM in two pairs of one-way-coupled Nd:YVO4 microchip lasers and realized two channels chaos-based optical communication. Argyris *et al.* [20] experimentally presented a dense-WDM (DWDM) optical chaos communication system and achieved 1.25 Gb/s encrypted data streams hidden propagation by using a distributed feedback semiconductor laser (DFB-SL) and two photonic monolithic integrated chaotic sources as transmitters. Though some progresses have been achieved in WDM chaos communication as mentioned above, there are still many key devices and techniques needed to be broken through if the WDM chaos communication can be seamless compatibility with existing commercial optical fiber transmission system. For constructing a flexible high-speed WDM chaos communication system, large-range wavelength-tunable chaotic carrier sources are crucial devices. However, current chaotic carrier sources based on commonly commercial DFB-SLs or vertical-cavity surface-emitting lasers (VCSELs) cannot meet relevant requirements since they can only be tuned within a very small range by adjusting the temperature or bias current. Besides, the chaotic carrier from such large-range wavelength-tunable chaotic carrier source should possess wide bandwidth to realize high-speed message transmission of optical chaos communications. Based on above considerations, designing and developing broadband large-range wavelength-tunable chaotic carrier sources become necessary to promote the development of WDM chaos communication technique.

In this Letter, we propose and experimentally demonstrate a broadband large-range wavelength-tunable chaotic carrier source by combining a weak-resonant-cavity Fabry-Perot laser diode (WRC-FPLD) [21], [22] with a filter. Compared with conventional FPLD, the front-facet of WRC-FPLD coats imperfect anti-reflection thus the WRC-FPLD can provide broader gain spectrum. Meanwhile, the length of the cavity of WRC-FPLD is longer than that of conventional FPLD, which means smaller longitudinal mode spacing and more WDM channels can be obtained [23]–[25]. Moreover, in order to realize the wavelength adjustability of the generated chaotic signal, a filtered optical feedback is adopted in this work. Previous studies have showed that the filtered optical feedback scheme introduces an externally controllable nonlinearity of the device and shows superiority in controlling the dynamical response of a laser [26]–[31]. In 1999, Yousefi and Lenstra [26] theoretically investigated the dynamics of a SL subject to weak filtered optical feedback for the first time, and the simulated results demonstrated that weak filter optical feedback can stabilize the system and suppress the low-frequency fluctuation for moderately broad
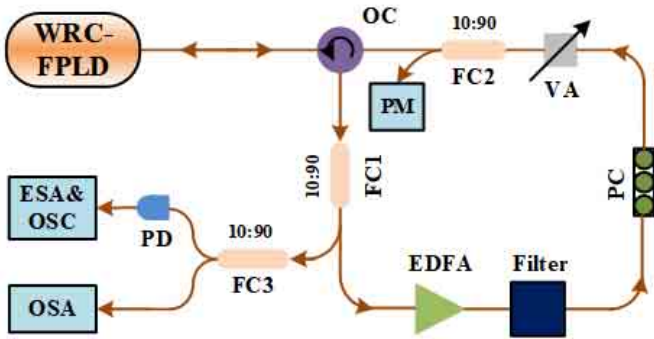
Fig. 1. Experimental setup. WRC-FPLD: weak-resonant-cavity Fabry-Perot laser diode; OC: optical circulator; FC: fiber coupler; EDFA: erbium-doped fiber amplifier; Filter: tunable optical filter; PC: polarization controller; VA: variable attenuator; PM: power meter; PD: photodetector; ESA: electrical spectrum analyzer; OSA: optical spectrum analyzer; OSC: oscilloscope.

filtered feedback. Subsequently, they further systematically investigated the nonlinear dynamical behaviors and hysteresis characteristics of a SL subject to delayed filtered optical feedback provided by a FP interferometer, and presented a complete physical scenario of filtered optical feedback properties [27]–[29]. Besides, gratings can also be used to provide a filtered optical feedback. For a SL subject to filtered optical feedback from a grating, chaotic emission has been observed [30]–[31]. In this work, via a commercial tunable filter to provide filtered optical feedback and an erbium-doped fiber amplifier (EDFA) to enhance the feedback, the wavelength of the chaotic output can be tuned within a relatively wide range depended on the tunable range of the filter. Furthermore, the chaotic bandwidth of each longitudinal mode within the tunable range of the filter is analyzed and the maximal chaotic bandwidth of each mode has been determined.

II. EXPERIMENTAL SETUP

Figure 1 shows the schematic diagram of experimental setup. A WRC-FPLD packaged with a fiber pigtail is used, and the bias current and temperature of the laser are controlled by an ultra-low noise and high accuracy current-temperature controller (ILX-Lightwave, LDC-3724B). The optical output of the WRC-FPLD firstly passes through an optical circulator (OC) and then is split into two parts by a fiber coupler (FC1). One part is amplified by an erbium doped fiber amplifier (EDFA), passes through a commercial tunable filter (AOS, tunable range: 1544.00 nm ∼ 1556.00 nm, 3dB bandwidth: 0.28 nm), and then fed back to the WRC-FPLD. The other part is sent to the detection system, which includes a photodetector (PD, U2T-XPDV3120R, 70 GHz bandwidth), an electrical spectrum analyzer (ESA, R&SFSW, 67 GHz bandwidth), an optical spectrum analyzer (OSA, Ando AQ6317C), and a digital oscilloscope (OSC, Agilent DSO-X 91604A, 16 GHz bandwidth). A polarization controller (PC) is used to control the polarization of the feedback light, and a variable attenuator (VA) is used to adjust the feedback power which is monitored by a power meter (PM). During the experiment, the temperature of the WRC-FPLD is stabilized at 20.02 ° C and the bias current is fixed at 35.00 mA.
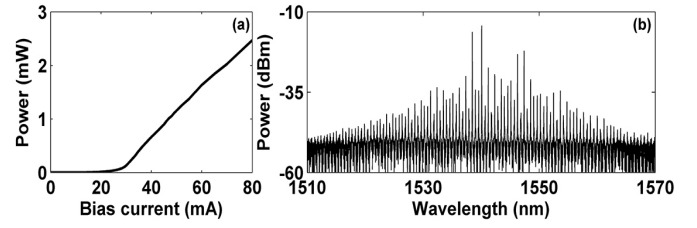

Fig. 2. L-I curve (a) of free-running WRC-FPLD and optical spectrum (b) of the laser biased at 35.00 mA.

III. EXPERIMENTAL RESULTS

Figure 2 measures the basic properties of the free-running WRC-FPLD. In Fig. 2(a), the experimentally recorded power-current curve is presented. As seen in this diagram, the threshold current I_{th} of the WRC-FPLD is about 27.80 mA. For a free-running WRC-FPLD, the losses of all modes are approximately identical, and then the distribution of net mode gain is only determined by the distribution of the gain supplied by the medium. When the bias current is located at a level just above the threshold, there are many modes existing in the laser due to very wide gain spectrum of the active medium in WRC-FPLD and very weak reflection of the front-facet of WRC-FPLD. Fig. 2(b) records the optical spectrum when the laser is biased at 35.00 mA, where more than 100 longitudinal modes with a mode interval of about 0.56 nm can be observed. However, after introducing a filtered feedback, different modes experience different losses. In particular, if the filtered feedback is strong enough and meanwhile the bandwidth of the filter is small enough, only one longitudinal-mode obtains much more gain than the others, and then single longitudinal-mode oscillation is realized. Through adjusting the central wavelength of the filter, it is possible to choose different mode to be the unique oscillation mode. As a result, the wavelength-tunability can be achieved. On this basis, through further selecting suitable feedback strength, the dynamics state of the WRC-FPLD can also be controlled. The corresponding experiment results show that after introducing a filtered feedback, the laser can be driven into chaos, and the central wavelength of the chaos output can be tuned within the tunable range of the filter (1544.00 nm ∼1556.00 nm), which is determined by the tuning range of the used filter in this work.

Firstly, the influence of the feedback power ξ_f on the chaotic bandwidth is investigated, where the chaotic bandwidth is estimated as the width of the band from zero to the frequency which contains 80% of signal energy after the noise floor has been removed. For simplification, in this work, the central wavelength of the filter is set at the resonant wavelength of chosen longitudinal mode of the free-running WRC-FPLD. Here, the longitudinal mode lasing at 1550.80 nm is selected as an example. Figure 3 displays optical spectra, corresponding power spectra and time series of the WRC-FPLD under different feedback power ξ_f, where the reflection spectrum of the filter has also been presented. When the WRC-FPLD is free-running (shown in Row 1), the power of each mode within the wavelength range from 1548.80 nm to 1552.80 nm is similar. The time series is nearly a constant level with small ripples due to the noise and the dynamical state is stable state. For $\xi_f = 0.41$ mW (Row 2), the longitudinal mode at 1550.80 nm is excited and the other modes are suppressed. The reason is that
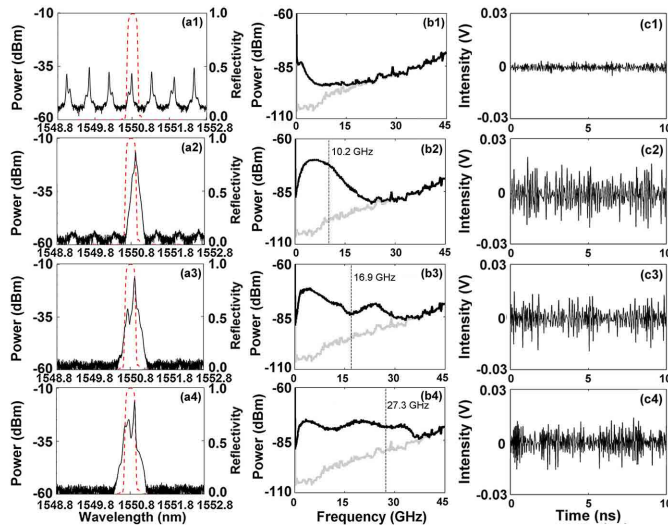
Fig. 3. (a) Optical spectra of the output from WRC-FPLD, (b) corresponding power spectra and (c) time series under $\xi_f = 0$ (Row 1), 0.41 mW (Row 2), 1.85 mW (Row 3) and 2.75 mW (Row 4), respectively, where the dashed red lines in the diagrams of left column are the reflection spectrum of the filter and the gray lines in power spectra denote the noise floor.

different from conventional mirrors, the tunable filter can provide wavelength-selective filtered reflection, and thus the longitudinal mode at 1550.80 nm gets more feedback power than the other longitudinal modes. Meanwhile, the optical spectrum (Fig. 3(a2)) of the mode is broadened obviously and the time series (Fig. 3(c2)) behaves dramatically fluctuation, which indicates that the laser has been driven into chaos. Also, the mode undergoes red-shift due to the filtered feedback. Furthermore, the measured power spectrum (Fig. 3(b2)) shows the power spectrum rapidly decreases to the noise floor (gray line) for the frequency is beyond 20.0 GHz, and the bandwidth of the chaotic output is about 10.2 GHz. Further increasing ξ_f to 1.85 mW, as shown in Row 3, the optical spectrum is further broadened and an extra peak emerges. The reason for further broadening optical spectrum is that the coherence collapsing of original longitudinal mode lasing at 1550.80 nm is more serious due to the stronger optical feedback. And, a dip observed at about 1550.78 nm, which is the origin of two peaks construction, may be resulted by that the anti-resonance phase condition is achieved. Correspondingly, a peak around 24.0 GHz in the power spectrum (Fig. 3(b3)) is observed, which corresponds the frequency interval between the two peaks emerging in the optical spectrum and the chaotic bandwidth is expanded to about 16.9 GHz. For $\xi_f = 2.75$ mW, as shown in row 4, the peak located at the shorter wavelength continues to rise and red-shift, and the whole optical spectrum is further broadened. Meantime, the power for the higher frequency components increases and the power spectrum becomes flatter, and the bandwidth of the chaotic output is enhanced dramatically and reaches 27.3 GHz.

Next, to further clarify the effect of ξ_f on the bandwidth of the chaotic signal output from the WRC-FPLD with filtered feedback, the chaotic bandwidth evolution with ξ_f is given in Fig. 4, where three different longitudinal modes are considered by adjusting the central wavelength of the filter. It should be pointed out that for $\xi_f < 0.35$ mW, the output of the WRC-FPLD is periodic oscillation, which is beyond the scope of this work. From Fig. 4, it can be seen that similar evolved
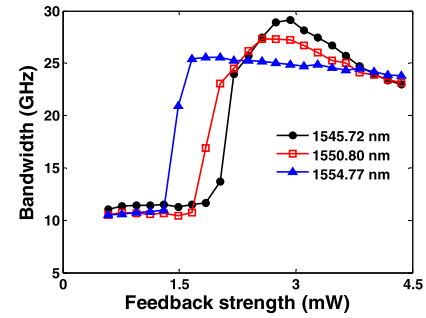

Fig. 4. Bandwidths of the chaotic outputs as a function of ξ_f for three different longitudinal modes of the WRC-FPLD.
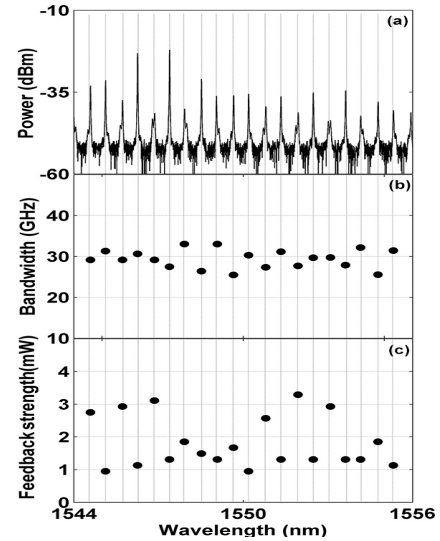

Fig. 5. (a) Optical spectrum of the solitary WRC-FPLD within the tunable range of the filter, (b) maximal chaotic bandwidth of each chosen longitudinal mode and (c) corresponding ξ_f.

trends are observed for the three different longitudinal modes, and then we take the longitudinal mode with the resonant wavelength of 1554.77 nm as an example to analyze the influence of ξ_f on the chaotic bandwidth. For a relatively low feedback power (0.35 mW $< \xi_f <$ 1.40 mW), the bandwidth of the chaotic output increases slowly and maintains a level about 10.0 GHz. With the further increase from $\xi_f = 1.40$ mW, the bandwidth rapidly increases and arrives at its maximum, and then decreases slowly within the measurement range. This can be explained as that, for 0.35 mW $< \xi_f <$ 1.40 mW, the feedback induced red-shift is relatively small, and the optical spectrum of the output remains a single-peak structure. Under this circumstance, the slow increase of the chaotic bandwidth with ξ_f is due to the gradual increase of the relaxation oscillation frequency resulted by the optical feedback. However, further increasing ξ_f from 1.40 mW will lead to a relatively large wavelength deviation between the longitudinal mode and the central wavelength of the filter, which results in an extra peak observed in the optical spectrum. Correspondingly, the beating between the original peak and the extra peak makes the power spectrum enhance around the beat frequency at about 20.0 GHz. Therefore, through selecting suitable ξ_f, the chaotic signal with large bandwidth can be obtained.

Finally, the chaotic bandwidths of each longitudinal mode within the tunable range of the filter are investigated respectively. Figure 5 presents optical spectrum of the solitary WRC-FPLD (a), maximal chaotic bandwidth of each chosen longitudinal mode (b) and corresponding ξ_f when the chaotic bandwidth reaches its maximum (c). As shown in Fig. 5(a), when the WRC-FPLD is free-running, there are twenty longitudinal modes within the tunable range of the filter from 1544.00 nm to 1556.00 nm. From Fig. 5(b), it can be observed that the maximal chaotic bandwidth of each chosen longitudinal mode can reach a level of about 30.0 GHz. However, from Fig. 5(c), the values of ξ_f for different longitudinal modes required to obtain the maximal bandwidths are different, which may attribute to the gain difference among the different longitudinal modes. As a result, to realize the chaos output with maximal chaotic bandwidth for every chosen longitudinal mode, the feedback power ξ_f needs to be carefully selected.

IV. Conclusion

In summary, wavelength-tunable broadband chaotic carrier generation from a WRC-FPLD subject to filtered feedback is proposed and experimentally demonstrated. The results show that, through adjusting the central wavelength of the filter and selecting suitable feedback power, about twenty longitudinal modes of the WRC-FPLD can be individually driven into chaos with bandwidth of about 30.0 GHz. Though the tunable range of the chaos carrier is about 10.00 nm limited by the tunable range of the filter, it can be expected that much more longitudinal modes of the WRC-FPLD can be driven into chaos and more large tunable range of the chaotic carrier can be achieved if a filter with a wider tunable range is used. We believe that this work will be helpful for multi-channel high-rate chaos optical communication.

References

[1] M. Sciamanna and K. A. Shore, "Physics and applications of laser diode chaos," *Nature Photon.*, vol. 9, no. 3, pp. 151–162, Mar. 2015.

[2] A. Uchida et al., "Fast physical random bit generation with chaotic semiconductor lasers," *Nature Photon.*, vol. 2, no. 12, pp. 728–732, Nov. 2008.

[3] X.-Z. Li, S.-S. Li, J.-P. Zhuang, and S.-C. Chan, "Random bit generation at tunable rates using a chaotic semiconductor laser under distributed feedback," *Opt. Lett.*, vol. 40, no. 17, pp. 3970–3973, Sep. 2015.

[4] X. Tang et al., "Tbits/s physical random bit generation based on mutually coupled semiconductor laser chaotic entropy source," *Opt. Exp.*, vol. 23, no. 26, pp. 33130–33141, Dec. 2015.

[5] F.-Y. Lin and J.-M. Liu, "Chaotic radar using nonlinear laser dynamics," *IEEE J. Quantum Electron.*, vol. 40, no. 6, pp. 815–820, Jun. 2004.

[6] C. R. Mirasso, P. Colet, and P. Garcia-Fernandez, "Synchronization of chaotic semiconductor lasers: Application to encoded communications," *IEEE Photon. Technol. Lett.*, vol. 8, no. 2, pp. 299–301, Feb. 1996.

[7] G. D. VanWiggeren and R. Roy, "Communication with chaotic lasers," *Science*, vol. 279, no. 5354, pp. 1198–1200, Feb. 1998.

[8] A. Argyris et al., "Chaos-based communications at high bit rates using commercial fibre-optic links," *Nature*, vol. 438, no. 7066, p. 343, Nov. 2005.

[9] J. Liu, Z.-M. Wu, and G.-Q. Xia, "Dual-channel chaos synchronization and communication based on unidirectionally coupled VCSELs with polarization-rotated optical feedback and polarization-rotated optical injection," *Opt. Exp.*, vol. 17, no. 15, pp. 12619–12626, Aug. 2009.

[10] Y. Hong, M. W. Lee, J. Paul, P. S. Spencer, and K. A. Shore, "GHz bandwidth message transmission using chaotic vertical-cavity surface-emitting lasers," *J. Lightw. Technol.*, vol. 27, no. 22, pp. 5099–5105, Nov. 15, 2009.

[11] J.-G. Wu, Z.-M. Wu, X. Tang, L. Fan, W. Deng, and G.-Q. Xia, "Experimental demonstration of LD-based bidirectional fiber-optic chaos communication," *IEEE Photon. Technol. Lett.*, vol. 25, no. 6, pp. 587–590, Mar. 15, 2013.

[12] M. Zhang, T. Liu, P. Li, A. Wang, J. Zhang, and Y. Wang, "Generation of broadband chaotic laser using dual-wavelength optically injected Fabry–Pérot laser diode with optical feedback," *IEEE Photon. Technol. Lett.*, vol. 23, no. 24, pp. 1872–1874, Dec. 15, 2011.

[13] S. Priyadarshi, I. Pierce, Y. Hong, and K. A. Shore, "Optimal operating conditions for external cavity semiconductor laser optical chaos communication system," *Semicond. Sci. Technol.*, vol. 27, no. 9, p. 094002, Sep. 2012.

[14] A. Elsonbaty, S. F. Hegazy, and S. S. A. Obayya, "Simultaneous suppression of time-delay signature in intensity and phase of dual-channel chaos communication," *IEEE J. Quantum Electron.*, vol. 51, no. 9, Sep. 2015, Art. no. 2400309.

[15] E. Mercier, D. Wolfersberger, and M. Sciamanna, "High-frequency chaotic dynamics enabled by optical phase-conjugation," *Sci. Rep.*, vol. 6, no. 6, Jan. 2016, Art. no. 18988.

[16] J.-Z. Zhang, A.-B. Wang, J.-F. Wang, and Y.-C. Wang, "Wavelength division multiplexing of chaotic secure and fiber-optic communications," *Opt. Exp.*, vol. 17, no. 8, pp. 6357–6367, Apr. 2009.

[17] N. Jiang, C. Xue, Y. Lv, and K. Qiu, "Physically enhanced secure wavelength division multiplexing chaos communication using multi-mode semiconductor lasers," *Nonlinear Dyn.*, vol. 86, pp. 1937–1949, Nov. 2016.

[18] J. Paul, S. Sivaprakasam, and K. A. Shore, "Dual-channel chaotic optical communications using external-cavity semiconductor lasers," *J. Opt. Soc. Amer. B, Opt. Phys.*, vol. 21, no. 3, pp. 514–521, Mar. 2004.

[19] T. Matsuura, A. Uchida, and S. Yoshimori, "Chaotic wavelength division multiplexing for optical communication," *Opt. Lett.*, vol. 29, no. 23, pp. 2731–2733, Dec. 2004.

[20] A. Argyris, E. Grivas, A. Bogris, and D. Syvridis, "Transmission effects in wavelength division multiplexed chaotic optical communication systems," *J. Lightw. Technol.*, vol. 28, no. 21, pp. 3107–3114, Nov. 1, 2010.

[21] G.-R. Lin, H.-L. Wang, T.-K. Cheng, and G.-C. Lin, "Suppressing chirp and power penalty of channelized ASE injection-locked mode-number tunable weak-resonant-cavity FPLD transmitter," *IEEE J. Quantum Electron.*, vol. 45, no. 9, pp. 1106–1113, Sep. 2009.

[22] G.-R. Lin, H.-L. Wang, G.-C. Lin, Y.-H. Huang, Y.-H. Lin, and T.-K. Cheng, "Comparison on injection-locked Fabry–Perot laser diode with front-facet reflectivity of 1% and 30% for optical data transmission in WDM-PON system," *J. Lightw. Technol.*, vol. 27, no. 14, pp. 2779–2785, Jul. 15, 2009.

[23] G.-R. Lin et al., "Long-cavity Fabry–Perot laser amplifier transmitter with enhanced injection-locking bandwidth for WDM-PON application," *J. Lightw. Technol.*, vol. 28, no. 20, pp. 2925–2932, Oct. 15, 2010.

[24] G.-H. Peng, J.-J. Kang, Y.-C. Lin, Y.-C. Chi, C.-K. Lee, and G.-R. Lin, "Chirp-compensated multichannel hybrid DWDM/TDM pulsed carrier from optically injection-mode-locked weak-resonant-cavity laser diode fiber ring," *IEEE J. Quantum Electron.*, vol. 47, no. 2, pp. 182–189, Feb. 2011.

[25] M.-C. Cheng, Y.-C. Chi, Y.-C. Li, C.-T. Tsai, and G.-R. Lin, "Suppressing the relaxation oscillation noise of injection-locked WRC-FPLD for directly modulated OFDM transmission," *Opt. Exp.*, vol. 22, no. 13, pp. 15724–15736, Dec. 2014.

[26] M. Yousefi and D. Lenstra, "Dynamical behavior of a semiconductor laser with filtered external optical feedback," *IEEE J. Quantum Electron.*, vol. 35, no. 6, pp. 970–976, Jun. 1999.

[27] A. P. A. Fischer, O. K. Andersen, M. Yousefi, S. Stolte, and D. Lenstra, "Experimental and theoretical study of filtered optical feedback in a semiconductor laser," *IEEE J. Quantum Electron.*, vol. 36, no. 3, pp. 375–384, Mar. 2000.

[28] M. Yousefi, D. Lenstra, G. Vemuri, and A. Fischer, "Control of nonlinear dynamics of a semiconductor laser with filtered optical feedback," *IEE Proc.-Optoelectron.*, vol. 148, no. 56, pp. 233–237, Oct./Dec. 2001.

[29] A. P. A. Fischer, M. Yousefi, D. Lenstra, M. W. Carter, and G. Vemuri, "Experimental and theoretical study of semiconductor laser dynamics due to filtered optical feedback," *IEEE J. Sel. Topics Quantum Electron.*, vol. 10, no. 5, pp. 944–954, Sep. 2004.

[30] E. C. Mos, G. W. T. Hooft, J. J. H. B. Schleipen, and H. D. Waardt, "Chaotic self-pulsation and cross-modulation in a wavelength-selective external-cavity laser diode," *IEEE J. Quantum Electron.*, vol. 37, no. 7, pp. 911–918, Jul. 2001.

[31] I. R. Andrei, "Characterization of chaotic emission of a laser diode in optical feedback conditions produced by different external reflectors," *Optoelectron. Adv. Mater.-Rapid Commun.*, vol. 4, no. 10, pp. 1440–1444, Oct. 2010.